Polycystins 1 and 2 mediate mechanosensation in the primary cilium of kidney cells

Surya M. Nauli[1*], Francis J. Alenghat[2], Ying Luo[1*], Eric Williams[1], Peter Vassilev[3], Xiaogang Li[1], Andrew E.H. Elia[1], Weining Lu[1], Edward M. Brown[3], Stephen J. Quinn[3], Donald E. Ingber[2] & Jing Zhou[1]

*These authors contributed equally to this work.

Published online: 6 January 2003; doi:10.1038/ng1076

Several proteins implicated in the pathogenesis of polycystic kidney disease (PKD) localize to cilia. Furthermore, cilia are malformed in mice with PKD with mutations in *TgN737Rpw* (encoding polaris). It is not known, however, whether ciliary dysfunction occurs or is relevant to cyst formation in PKD. Here, we show that polycystin-1 (PC1) and polycystin-2 (PC2), proteins respectively encoded by *Pkd1* and *Pkd2*, mouse orthologs of genes mutated in human autosomal dominant PKD, co-distribute in the primary cilia of kidney epithelium. Cells isolated from transgenic mice that lack functional PC1 formed cilia but did not increase Ca^{2+} influx in response to physiological fluid flow. Blocking antibodies directed against PC2 similarly abolished the flow response in wild-type cells as did inhibitors of the ryanodine receptor, whereas inhibitors of G-proteins, phospholipase C and $InsP_3$ receptors had no effect. These data suggest that PC1 and PC2 contribute to fluid-flow sensation by the primary cilium in renal epithelium and that they both function in the same mechanotransduction pathway. Loss or dysfunction of PC1 or PC2 may therefore lead to PKD owing to the inability of cells to sense mechanical cues that normally regulate tissue morphogenesis.

Introduction

Autosomal dominant PKD is a common lethal monogenic disorder, characterized by progressive development of fluid-filled cysts in the kidney. Mutations in *PKD1* and *PKD2*, which respectively encode integral membrane proteins PC1 and PC2, account for all cases of autosomal dominant PKD[1–3]. PC1 activates a G-protein signaling pathway by binding and activating heterotrimeric Gαi/o proteins[4,5], which, in turn, modulate voltage-gated Ca^{2+} and K^+ channels[5]. PC2 functions as a Ca^{2+}-permeable cation channel[6–9]. PC1 and PC2 are known to heterodimerize[3,5,10]. The mechanism by which mutations in *PKD1* and *PKD2* lead to abnormal kidney development, however, is yet unclear.

One clue to the pathogenesis of PKD is that, in addition to PC2, two other proteins, cystin and polaris, mutant forms of which are also associated with PKD[11,12], localize to the primary cilium of renal epithelial cells[12–14]. A cilium is a tiny hair-like appendage about 0.25 μm in diameter that contains a microtubule bundle as a core. Cilia, which extend from the surfaces of many cell types and are found in many species, contribute to fluid movement[15], chemoreception[16] and patterning of the left–right body axis[17]. The primary cilium is a non-motile cilium with a microtubule arrangement of 9+0; it is unique in that, in almost all cases, only one primary cilium is expressed on the apical surface of each epithelial cell. Kidney epithelial cells have well developed primary cilia that extend into the tubular lumen. The integrity of cilia in mice with mutations in *Pkd2* is unknown, but shortened cilia have been found in renal tubules of mice with mutations in *TgN737Rpw*[18]. Mice with mutations in *TgN737Rpw* or *Pkd2* develop defects in left–right symmetry[19,20] in addition to PKD.

Although several proteins involved in PKD pathogenesis are expressed in cilia, it is not clear whether or how ciliary dysfunction results in abnormal kidney development and cyst formation. The contribution of PC1 to cilium function is not known. Recent work has shown that the primary cilium of the kidney epithelium mediates sensation of mechanical signals produced by apical fluid shear stress and its transduction into an intracellular Ca^{2+}

[1]*Renal Division, Department of Medicine, Brigham and Women's Hospital and Harvard Medical School, 4 Blackfan Circle, Boston, Massachusetts 02115, USA.* [2]*Vascular Biology Program, Departments of Pathology and Surgery, Children's Hospital and Harvard Medical School, Boston, Massachusetts, USA.* [3]*Endocrine-Hypertension Division, Department of Medicine, Brigham and Women's Hospital and Harvard Medical School, Boston, Massachusetts, USA. Correspondence should be addressed to J.Z. (e-mail: zhou@rics.bwh.harvard.edu).*

signaling response[21]. Fluid shear stress is known to regulate tissue morphogenesis and, in particular, lumen diameter in the vasculature[22,23]. Thus, we explored whether PC1 co-distributes with PC2 in the primary cilium of kidney epithelium and whether these polycystins collectively contribute to mechanosensation in renal epithelial cells cultured from mice with targeted mutations in *Pkd1* and in cells from their wild-type littermates.

Results

Localization of PC1 in mice with mutations in *Pkd1*

To explore the role of cilia in human cystic disease and the potential function of PC1 in the cilium, we localized PC1 in kidneys from wild-type mice and mice homozygous with respect to a targeted deletion of exon 34 (*Pkd1*^{tm1Jzh}; herein called *Pkd1*$^{del34/del34}$ mice) at embryonic day (E) 15.5. This is the stage at which cysts are first seen in mice with mutations in *Pkd1*, most of which die during late gestation[24,25]. PC1 co-localized with the specific ciliary axoneme marker acetylated α-tubulin in kidneys of wild-type but not *Pkd1*$^{del34/del34}$ mice (Fig. 1*a*). Because cells develop longer, more visible cilia in culture than *in vivo*, we carried out similar immunolocalization studies in cells isolated from embryonic kidneys on the basis of their expression of the collecting-tubule marker *Dolichos biflorus* agglutinin (DBA; ref. 26). We confirmed the purity of these cell populations by fluorescence-activated cell sorting (Fig. 1*b*). The collecting tubule is a common site for cyst development[2,24,25,27] with high levels of expression of PC1 and other polycystins[27–29]. Homozygous *Pkd1*$^{del34/del34}$ mutants develop cysts in the collecting tubules at E17.5; thus, the cells we isolated at E15.5 were at a pre-cystic stage.

The DBA-positive epithelial cells that we isolated exhibited well developed cilia when fully differentiated for 3–4 days in culture. Analysis of these cells using a highly specific, affinity-purified antibody against PC1 confirmed that PC1 co-distributed with acetylated α-tubulin in wild-type but not *Pkd1*$^{del34/del34}$ cells (Fig. 1*c*). We detected only cytosolic PC1 staining in mutant cells, consistent with previous studies that have shown that dysfunctional PC1 is expressed in these cells[25]. Further analysis with γ-tubulin, a specific marker of the basal body of the cilium, also showed co-localization of PC1 in the basal body in wild-type but not in *Pkd1*$^{del34/del34}$ cells (Fig. 1*d*). Thus, PC1 seems to be a component of the primary cilium.

Cells with mutations in *Pkd1* do not activate flow-induced Ca^{2+} signaling

The primary cilium of kidney epithelium has recently been shown to mediate transduction of a mechanical flow stimulus into a Ca^{2+} signaling response[21], but the molecules that mediate this process have not been identified. To explore whether ciliary PC1 could contribute to this response, we used fluid shear stress to promote cilium bending and associated Ca^{2+} signaling in cultured kidney epithelial cells. Wild-type cells were loaded with the Ca^{2+}-binding dye Fura-2, exposed to the abrupt onset of fluid shear (0.75 dyne cm^{-2}) and analyzed by microfluorimetric ratio-imaging. On fluid stimulation, we detected an immediate rise in intracellular Ca^{2+} (from 144 ± 6 nM to 426 ± 59 nM; $n = 30$; $P < 10^{-6}$) throughout the cell population, peaking roughly 10–20 s after stimulation (Fig. 2*a*,*b*). Ca^{2+} levels then rapidly decreased but were maintained at moderate levels for 40–50 s before returning to base line; this response may be due to intercellular communication through specialized gap junctions[21]. The Ca^{2+} response induced by flow in these mouse embryonic kidney epithelial cells was faster than that observed in an established canine kidney epithelial cell line[21]; this difference may be due to differences in the cell types, species or experimental conditions used for flow stimulation. Notably, when we exposed mutant cells that lacked PC1 to an identical flow stimulus, we detected little or no Ca^{2+} influx (from

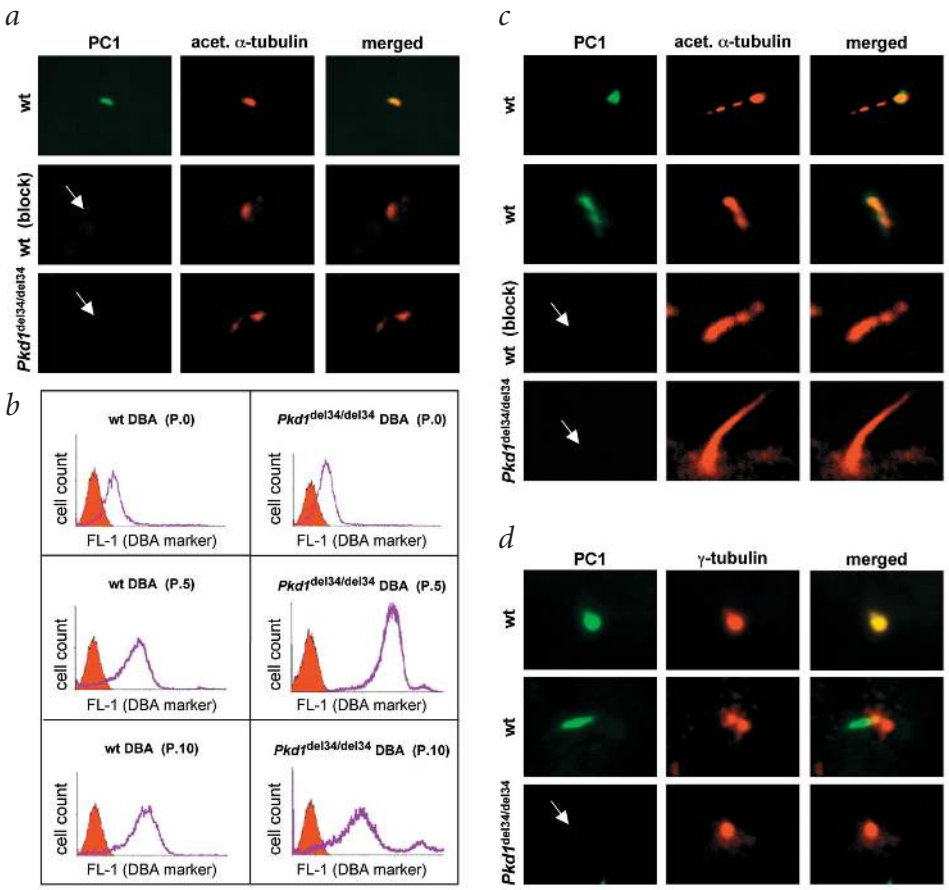

Fig. 1 Polycystin-1 was detected in the cilia of wild-type (wt) mouse embryonic kidney and collecting duct–derived epithelial cells. ***a***, PC1 (green) co-localized with a ciliary marker (acetylated α-tubulin, red) as indicated when a dual-channel filter was used (yellow). The subcellular localization of PC1 in wild-type kidneys with and without PC1-blocking peptide and in *Pkd1*$^{del34/del34}$ kidneys is shown. ***b***, Isolation of epithelia of collecting-duct origin using DBA as a marker. FL-1 denotes DBA fluorescence intensity. The expressions of membrane markers were examined before sorting (P.0) and after sorting at the fifth (P.5) and tenth (P.10) passages. ***c***, When acetylated α-tubulin was used as a ciliary marker, PC1 clearly appeared in the basal body and the trunk of the cilia of wild-type but not mutant cells. Blocking peptides were used in wild-type cells to show antibody specificity. ***d***, Co-localization of PC1 with γ-tubulin, a marker for the basal body of cilia, was seen in wild-type but not mutant cells. Original objective magnification: ×100.

154 ± 7 nM to 163 ± 4 nM; $n = 30$; $P > 0.1$) in either the early or late phase (Fig. 2*a*,*b*). Wild-type cells showed a specific sensitivity to low levels of shear stress similar to those observed in proximal tubules (about 1 dyne cm^{-2}; ref. 30) and other renal tubules (0.71 dyne cm^{-2}; ref. 21) *in vivo*. We did not observe Ca^{2+} signaling in wild-type or mutant cells when we applied higher levels of shear stress (15 dyne cm^{-2}).

Ca^{2+} entry is required to initiate flow-induced Ca^{2+} signaling

To study whether the flow-induced Ca^{2+} increases were due to an influx of extracellular Ca^{2+} or to release from intracellular Ca^{2+} stores, we repeated the experiment in medium depleted of Ca^{2+}. Under these conditions, the wild-type cells showed no response to flow (Fig. 2*c*), indicating that the mechanosensory response was mediated by Ca^{2+} influx across the plasma membrane.

To rule out the possibility that the mutant cells simply lost their general ability to carry out Ca^{2+} signaling, we stimulated the cells with a chemical receptor agonist, thrombin. Both wild-type and PC1-deficient cells responded to thrombin by increasing cytosolic Ca^{2+} concentrations (Fig. 2*d*,*f*). Thus, PC1-deficient cells retained the ability to conduct Ca^{2+} but lost the ability to sense fluid flow. When we did the same study in the absence of extracellular Ca^{2+} (Fig. 2*e*,*f*), we found that intraorganellar Ca^{2+} buffering had a more important role in thrombin-induced activation than in flow-induced activation of Ca^{2+} signaling. In fact, the Ca^{2+} response to thrombin was significantly greater in cells that lacked PC1 than in wild-type cells, either in the presence of extracellular Ca^{2+} (peak: 200 ± 27 nM in wild-type cells versus 295 ± 40 nM in mutant cells; $n = 16$ each; $P < 10^{-4}$) or in its absence (peak: 175 ± 10 nM in wild-type cells versus 232 ± 24 nM in mutant cells; $n = 15$ each; $P < 0.01$). There was no statistical difference in basal resting Ca^{2+} concentrations between the groups (Fig. 2*g*).

The primary cilium is required for flow-induced Ca^{2+} signaling

To verify that the Ca^{2+} response to mechanical flow was due to cilium activation, we carried out similar studies under growth conditions that inhibit cilium formation in wild-type cells (Fig. 3*a*–*c*). The collecting-duct epithelial cells differentiated and formed well developed cilia after 3–4 days in culture (Fig. 3*d*). In contrast, cells that were cultured for only 1 day in medium that promotes differentiation (Fig. 3*b*) or cultured in medium that promotes cell division (Fig. 3*f*) developed either short cilia or no cilia at all (Fig. 3*e*) with occasional expression of PC1. Con-

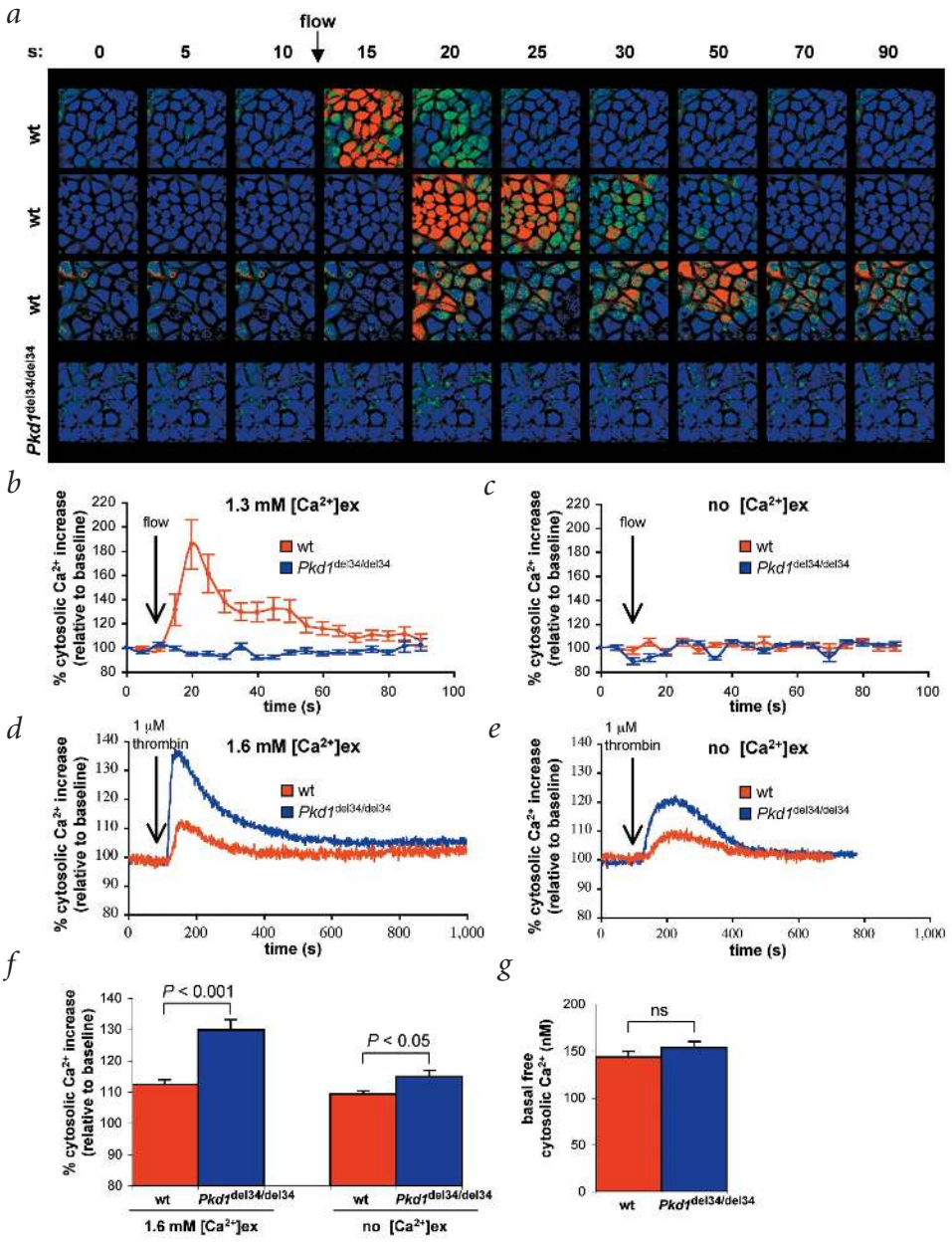

Fig. 2 Polycystin-1 mediated mechanical flow–induced extracellular Ca^{2+} influx. ***a***, A temporal representation of cytosolic Ca^{2+} responses to mechanical flow in three wild-type (wt) and one *Pkd1*$^{del34/del34}$ cell populations in the presence of extracellular Ca^{2+}. In most cases, the response peaked about 10 s after the flow was applied. Original objective magnification: ×20. ***b***,***c***, The averages of flow-induced changes in cytosolic Ca^{2+} for both wild-type (wt) and *Pkd1*$^{del34/del34}$ cells in the presence (*b*; $n = 30$ for each genotype) or absence (*c*; $n = 18$ for wild-type; 12 for *Pkd1*$^{del34/del34}$) of extracellular Ca^{2+}. ***d***,***e***, Compared with wild-type (wt) cells, *Pkd1*$^{del34/del34}$ cells had a greater Ca^{2+} response to 1 μM thrombin agonist in the presence (*d*) or absence (*e*) of extracellular Ca^{2+}. ***f***, The peaks of cytosolic Ca^{2+} relative to baseline Ca^{2+} level were averaged for both wild-type (wt) and *Pkd1*$^{del34/del34}$ cells in the presence ($n = 16$ for each genotype) or absence ($n = 15$ for each genotype) of extracellular Ca^{2+}. ***g***, Baseline cytosolic Ca^{2+} levels between wild-type (wt) and *Pkd1*$^{del34/del34}$ cells were compared ($n = 27$ for each genotype).

sistently, the flow-induced peak cytosolic Ca^{2+} levels were significantly lower in both partially differentiated cells (165 ± 3 nM; $n = 6$; $P < 0.05$) and proliferating cells (164 ± 9 nM; $n = 6$; $P < 0.05$) than in fully differentiated cells at 4 days with well developed cilia (366 ± 74 nM; $n = 6$). These observations suggest that PC1 must be present for a well formed cilium to sense flow and produce a Ca^{2+} signaling response. We did not observe a significant difference in cilia length between wild-type (12.2 ± 0.5 μm; $n = 184$) and mutant cells (12.8 ± 0.7 μm; $n = 83$) in their fully differentiated state.

Ca^{2+} entry through PC2 initiates flow-induced Ca^{2+} signaling

Because PC2 is a Ca^{2+}-permeable cation channel[7,8] and a binding partner of PC1 (refs. 3,10), we evaluated its role in flow-induced Ca^{2+} influx. In agreement with some recent findings[13], we found that PC2 co-localized with acetylated α-tubulin (Fig. 4*a*), γ-tubulin (Fig. 4*b*) and PC1 (Fig. 4*c*) in wild-type cells, but not in *Pkd1*$^{del34/del34}$ cells. To examine the functional importance of PC2 in mediating the cellular response to flow, we used various antibodies raised against PC1 and PC2 (Fig. 5*a*) in wild-type cells. Consistent with the results obtained from the mutant cell experiments, an antibody raised against PC1 (Fig. 5*b*) blocked the normal response of wild-type cells to flow stimulation. Application of antibody against the extracellular domain of PC2 also completely prevented flow-induced Ca^{2+} influx (Fig. 5*d*,*e*), whereas treatment with a control antibody against the intracellular domain of PC2 (p96525) had no effect (Fig. 5*c*). We verified the specificities of the antibodies against PC1 and PC2 using inducible 293T cell lines stably overexpressing PC1 or PC2 as well as electrophysiological analyses of PC2 channels in wild-type cells (Fig. 6).

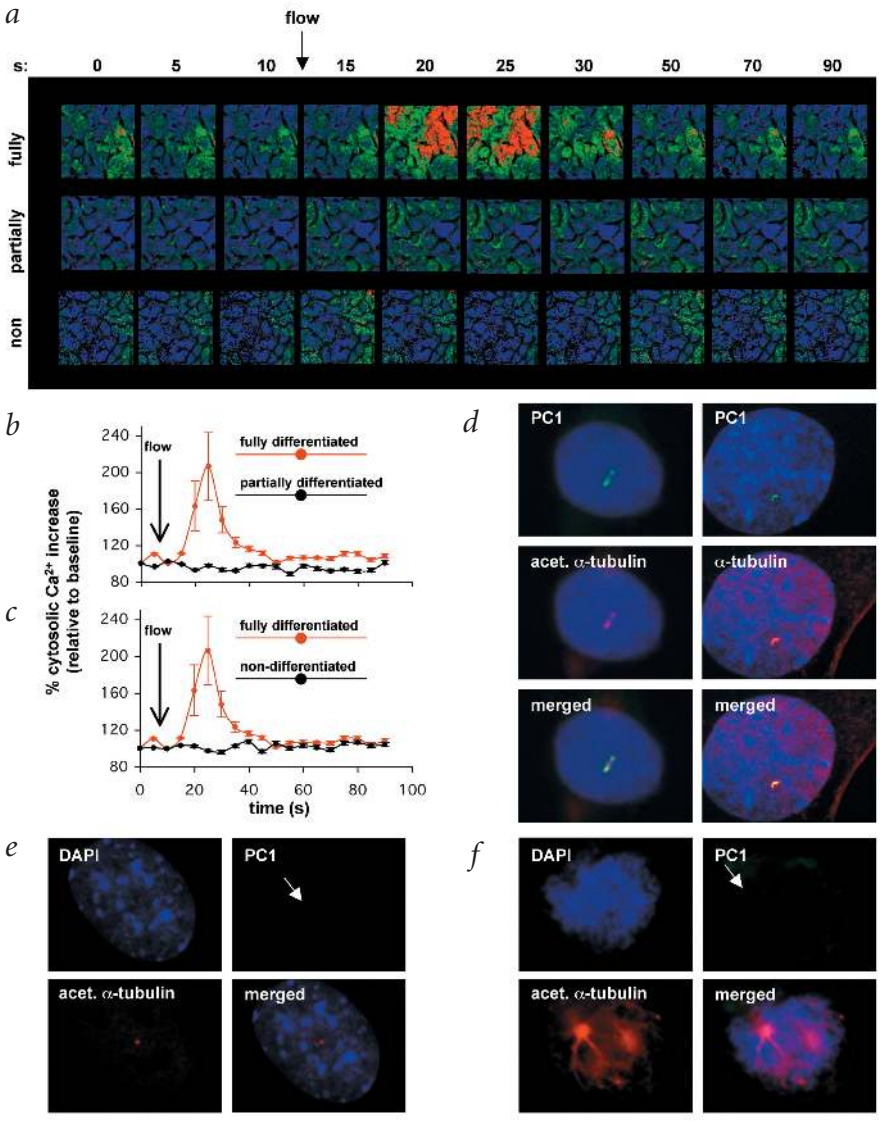

Fig. 3 Responses to mechanical flow stimulation require fully developed cilia. ***a***, A temporal pseudocolor of cytosolic Ca^{2+} response to flow stimulation in fully differentiated (control), partially differentiated (12–24 h) and non-differentiated cells. ***b***,***c***, Averaged Ca^{2+} responses to flow in partially differentiated (*b*) and non-differentiated (*c*) cells were compared with a control group ($n = 6$ each). ***d***–***f***, Double labeling of PC1 (green) with either acetylated α-tubulin or α-tubulin (red) in fully differentiated cells (*d*), in poorly differentiated cells that had short or no cilia (*e*) and in cells grown in the proliferation medium (*f*). PC1 was occasionally detected in cilia of poorly differentiated cells but never in cells grown in the proliferation media. Blue, DAPI (4′-6-diamidino-2-phenylindole) staining of cell nuclei. In some cases, cells in mitotic phase were observed (*f*).

Ca^{2+} influx induces intraorganellar Ca^{2+} release mediated by ryanodine receptors

To explore whether the influx of Ca^{2+} through PC2 triggered intraorganellar Ca^{2+} release, we examined whether ryanodine or $InsP_3$ receptor channels were involved in the response (Fig. 7*a*). We used a high concentration of caffeine to block ryanodine receptors and to empty intraorganellar Ca^{2+} pools sensitive to ryanodine[31]. We also used ryanodine to specifically block ryanodine receptors, which in turn would inhibit Ca^{2+}-induced Ca^{2+} release[31]. Caffeine (Fig. 7*b*) and ryanodine (Fig. 7*c*) each blocked the increase in cytosolic Ca^{2+} in response to flow in Ca^{2+}-containing medium. The peak increases in cytosolic Ca^{2+} were 187 ± 5 nM in cells treated with ryanodine ($P < 0.005$; $n = 12$) and 177 ± 4 nM in cells treated with caffeine ($P < 0.01$; $n = 6$) compared with 461 ± 76 nM in control cells ($n = 12$). Thus, release of intracellular Ca^{2+} through ryanodine receptors had an important role in polycystin-mediated flow-induced signaling in these embryonic kidney cells.

To explore the possibility that $InsP_3$ receptors were also involved in flow-induced intraorganellar Ca^{2+} release, we carried out similar studies using cells treated with selective inhibitors of G-proteins, phospholipase C and $InsP_3$ receptors (GDPβS, U73122 and 2-APB, respectively). None of these chemicals had a statistically significant effect on flow-induced cytosolic Ca^{2+} signaling relative to controls (Fig. 7*d*–*f*). The peak levels of cytosolic Ca^{2+} for the control groups and those treated with

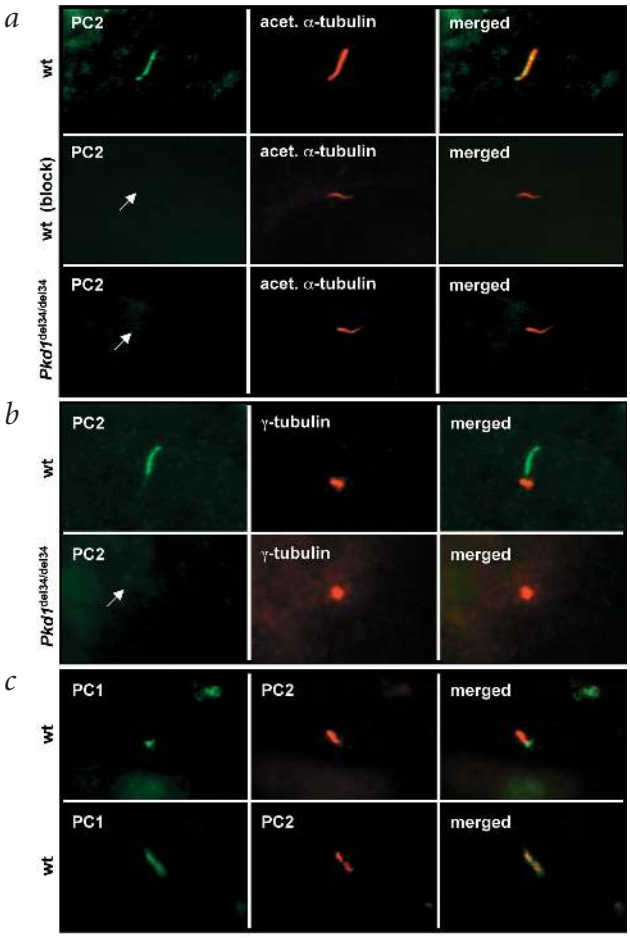

Fig. 4 Polycystin-2 was detected in the cilia of wild-type (wt) collecting duct–derived epithelial cells. ***a***, PC2 clearly appeared to co-localize with acetylated α-tubulin in wild-type but not in mutant cells. Blocking peptides were used in wild-type cells to show antibody specificity. ***b***, Double labeling of PC2 with γ-tubulin, a marker for the basal body of cilia. PC2 signal was seen in the wild-type but not mutant cells. ***c***, Co-distribution of PC1 and PC2 was observed in two wild-type cells. Original objective magnification: ×100.

GDPβS, U73122 or 2-APB were 494 ± 51 nM ($n = 12$), 506 ± 71 nM ($n = 12$), 413 ± 53 nM ($n = 6$) and 441 ± 42 nM ($n = 12$), respectively ($P > 0.5$ for all versus control).

Discussion

Collectively, our data indicate that ciliary PC1 and PC2 act in concert with ryanodine receptors to mediate transduction of an extracellular mechanical stimulus into a Ca^{2+} signaling response inside kidney epithelial cells. The requirement for extracellular Ca^{2+} indicates that the initial response to mechanical stimulation is the influx of Ca^{2+} across the plasma membrane, whereas the results obtained with ryanodine and caffeine suggest that the intraorganellar Ca^{2+} buffering system may mediate downstream signaling. Heterologous expression of PC2 alone has been known to result in augmented intraorganellar Ca^{2+} release[8,9], but PC2 channels can also be translocated to the plasma membrane in the presence of proteosome inhibitors and PC1 (refs. 8,10).

In this study, we found expression of both PC1 and PC2 on the cilia of mouse embryonic kidney cells and antibodies specific for PC2 appeared to block Ca^{2+} entry, suggesting a predominant role of PC2 in flow-induced Ca^{2+} influx, at least in these cells. We therefore propose that PC1, with its large extracellular domain[32], may sense the bending of the primary cilium induced by fluid flow, functioning as a mechano-fluid stress sensor. Resultant conformational changes of PC1 transduce the mechanical signal into a chemical response by activating tightly associated PC2 Ca^{2+} channels. This local Ca^{2+} influx in the cilium subsequently triggers intraorganellar Ca^{2+} release inside the cytoplasm through Ca^{2+}-induced Ca^{2+} release (Fig. 8). Changes in intracellular Ca^{2+} concentration may then alter various cell functions, including gene expression, growth, differentiation and apoptosis, thus altering tissue and organ development.

It is notable that, compared with normal epithelia, cells with mutations in *Pkd1* have greater intracellular Ca^{2+} responses to thrombin stimulation. The underlying mechanisms for this are currently unknown. Thrombin receptors are typical seven-transmembrane G-protein-coupled receptors[33,34] and may be coupled to Gi in epithelial cell lines[34]. PC1 also has been shown to act as an activator of heterotrimeric Gi and Go proteins that, in turn, regulate the activities of plasma membrane cation channels through the release of Gβγ subunits[5]. The flow-induced cytosolic Ca^{2+} increase does not seem to be mediated by G-proteins, however, as inhibitors of G-proteins had no effect on this process. This is consistent with our previous finding that the activation of G-proteins by PC1 is antagonized by PC2 when PC1 and PC2 are co-expressed[5]. The augmented Ca^{2+} signaling

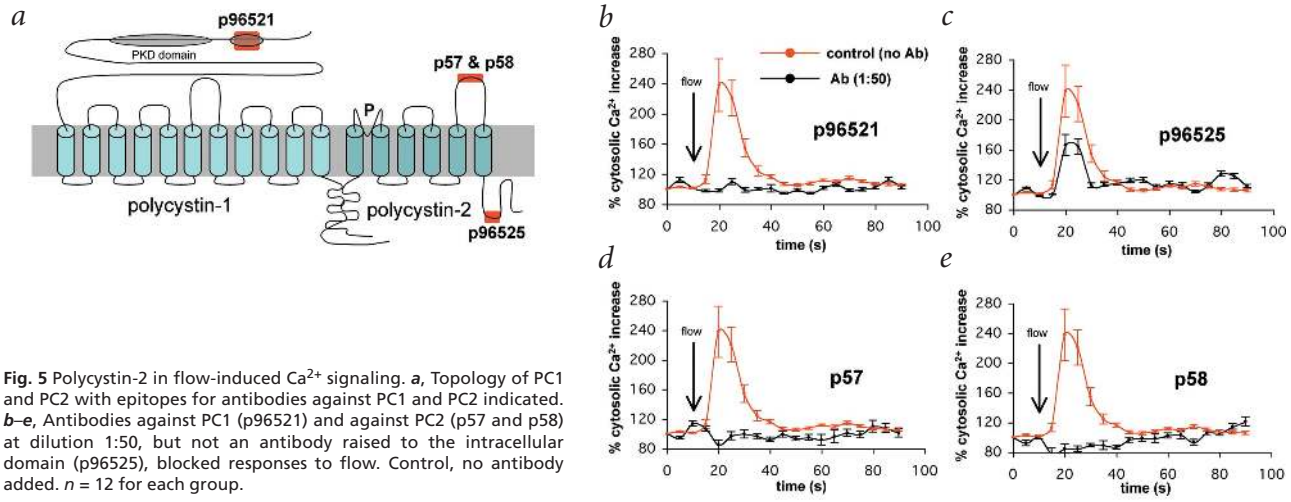

Fig. 5 Polycystin-2 in flow-induced Ca^{2+} signaling. ***a***, Topology of PC1 and PC2 with epitopes for antibodies against PC1 and PC2 indicated. ***b***–***e***, Antibodies against PC1 (p96521) and against PC2 (p57 and p58) at dilution 1:50, but not an antibody raised to the intracellular domain (p96525), blocked responses to flow. Control, no antibody added. $n = 12$ for each group.

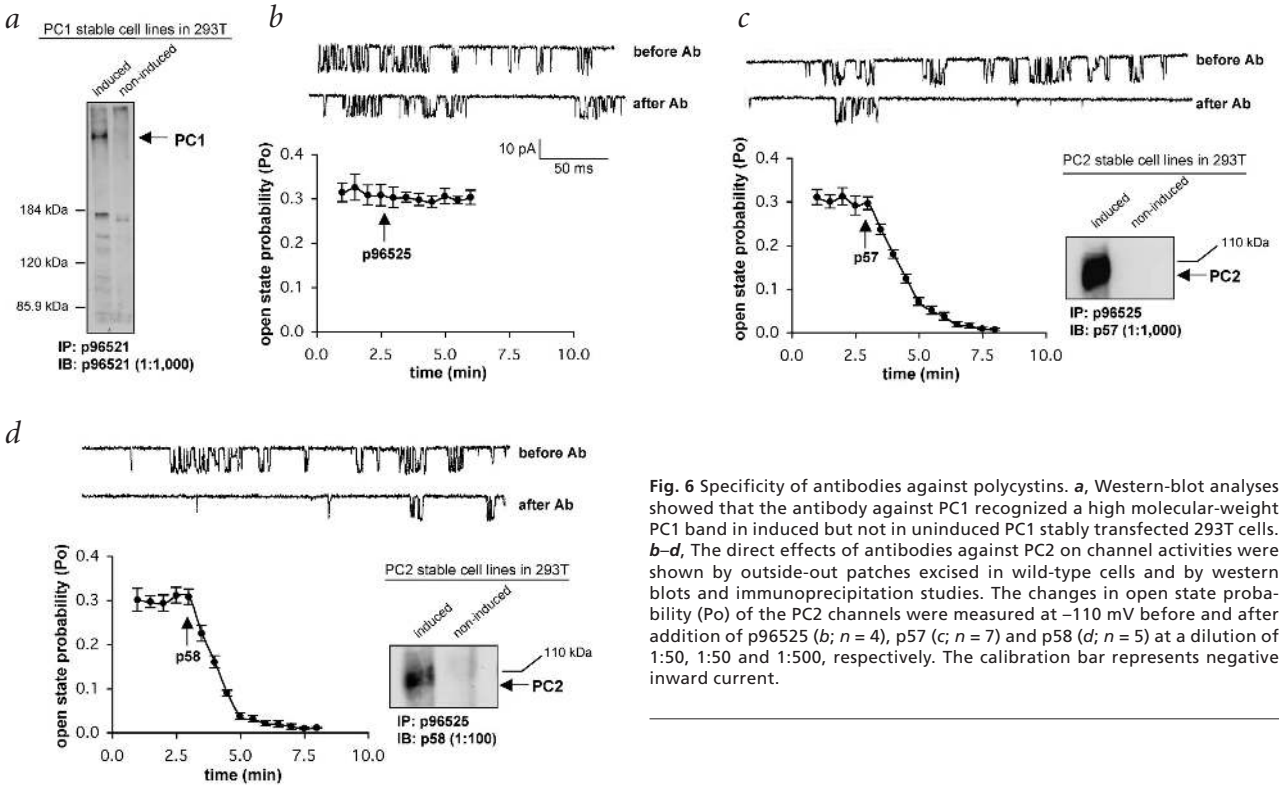

Fig. 6 Specificity of antibodies against polycystins. ***a***, Western-blot analyses showed that the antibody against PC1 recognized a high molecular-weight PC1 band in induced but not in uninduced PC1 stably transfected 293T cells. ***b–d***, The direct effects of antibodies against PC2 on channel activities were shown by outside-out patches excised in wild-type cells and by western blots and immunoprecipitation studies. The changes in open state probability (Po) of the PC2 channels were measured at –110 mV before and after addition of p96525 (*b*; $n = 4$), p57 (*c*; $n = 7$) and p58 (*d*; $n = 5$) at a dilution of 1:50, 1:50 and 1:500, respectively. The calibration bar represents negative inward current.

response to thrombin observed in the mutant cells may therefore reflect an imbalance in G-protein signaling due to mutant PC1 which, in turn, promotes enhanced Ca^{2+} release or transport by means of a different molecular pathway. We have also shown that PC1 does not activate Gq[5], a G-protein involved in intraorganellar Ca^{2+} release through the $InsP_3$ receptor. Consistent with these results, we found no evidence for the involvement of the $InsP_3$ receptor in response to flow.

Since the *Pkd1*^{del34} mouse model was generated[24], several mouse models with mutations in *Pkd1* have been established[25,35–37]. The phenotype associated with the *Pkd1*^{del34} mutation is similar to but slightly milder[25,37] than those associated with other *Pkd1* mutations in terms of kidney and pancreatic cysts, perinatal lethality, hydrops fetalis and polyhydroamnios in the homozygotes[24,25] and liver disease in the heterozygotes[38]. The relatively mild phenotype seems to be a mutation-specific effect that may be related to high levels of mutant PC1 in *Pkd1*$^{del34/del34}$ mice; high levels of PC1 are also found in kidneys of many individuals with autosomal dominant PKD[28,39,40]. Recent genotype–phenotype correlation studies in individuals with PKD also showed that 5′ *PKD1* mutations seem to result in more severe phenotypes than do 3′ mutations[41]. Some extrarenal phenotypes, such as hemorrhage and congestive heart failure, have been found only in some mice with mutations in *Pkd1*, which may be due to the nature of the mutation and the specific background mouse strains. In view of the data presented here, we

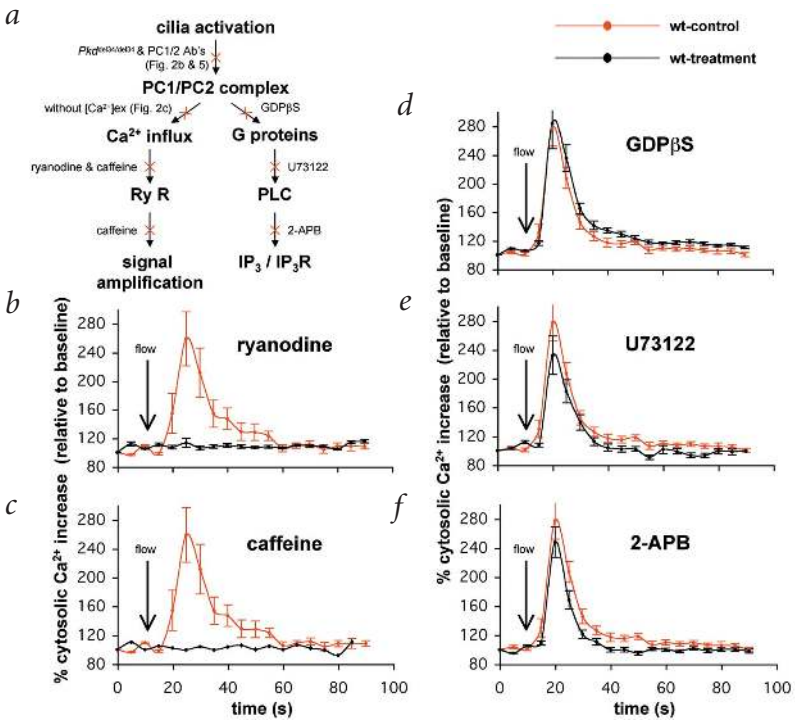

Fig. 7 Ca^{2+}-induced Ca^{2+} release was required for flow-induced Ca^{2+} responses. Two pathways that lead to intraorganellar Ca^{2+} release were examined (***a***). Parallel experiments on fluid shear stress with and without treatment of caffeine (***b***) or ryanodine (***c***) showed that emptying the ryanodine-sensitive pool or inhibition of ryanodine receptors (RyR), which are activated by increases in the cytosolic Ca^{2+} concentration under normal physiological conditions, significantly inhibited increases of cytosolic Ca^{2+} in response to flow. ***d–f***, Inhibitors of heterotrimeric G-proteins (*d*), phospholipase C (*e*) or $InsP_3$ receptors (*f*) did not inhibit the Ca^{2+} signal. $n = 6$ for caffeine and U73122 treatments; $n = 12$ for all others.

propose that the inability to respond to flow contributes to cyst formation but that alteration in other downstream or parallel signaling pathways may be responsible for modification of the phenotypes.

Polaris and cystin, which are mutated in two mouse models for PKD that are not related to human disease, have recently been localized to primary cilia in cultured renal epithelia[12,14,18]. Although the function of cystin is unknown, polaris seems to be critical for ciliogenesis, as mice with mutant polaris develop shortened cilia or no cilia in kidney epithelia. In light of our finding that cells with mutant PC1 are seemingly normal but do not sense fluid flow, we propose that the structural and functional integrity of the primary cilium is critical for normal kidney cell differentiation and organ morphogenesis. Defects in either may be key events in tubule dilatation and cyst formation. The mechanism behind this developmental control may be analogous to the mechanism by which normal blood vessels sense fluid shear stress and spontaneously remodel the vascular wall and change the lumen diameter to maintain a nearly constant fluid shear stress throughout the vasculature[22,23]. Similarly, cells that lack PC1 and flow-induced Ca^{2+} influx may respond as if the stress levels were constitutively high, resulting in tissue remodeling and a compensatory increase in the diameters of renal tubules and other ciliated ducts[1,2] (biliary and pancreatic), which are the cardinal features of PKD.

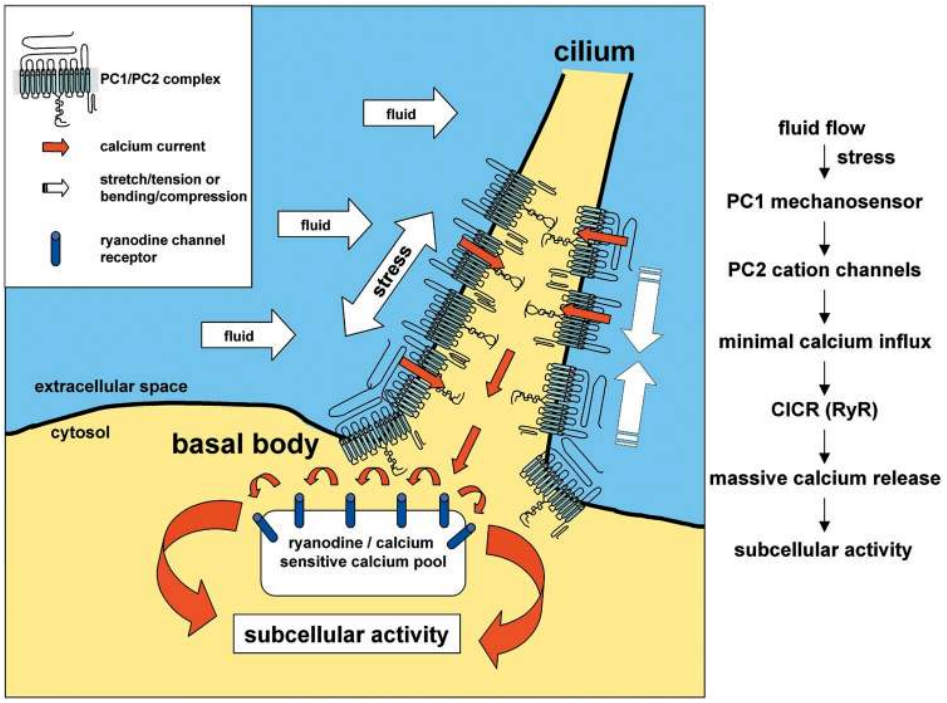

Fig. 8 Schematic diagram of mechanisms of fluid shear stress and Ca^{2+} signaling in mouse embryonic kidney cells. Cilia act as antennae to sense fluid movement. PC1, with its large extracellular domains, acts as a sensory molecule for fluid shear stress that transmits the signal from the extracellular fluid environment to PC2, which, in turn, produces sufficient Ca^{2+} influx to activate intracellular ryanodine receptors (RyR) through Ca^{2+}-induced Ca^{2+} release (CICR). The resulting local increase in the cytosolic Ca^{2+} concentration then regulates numerous molecular activities inside the cell that contribute to tissue development.

Methods

Embryonic kidney cell culture. We generated timed pregnancies by intercrossing mice heterozygous with respect to both the *Pkd1*^{del34} allele[24] and the temperature-sensitive SV40 large T antigen (Charles River). As described previously[24,25], *Pkd1*^{del34} was created by replacing exon 34 of *Pkd1* with a neomycin resistance gene, which results in a frame shift shortly after exon 33. This mutation is predicted to result in a truncated PC1 protein of 3,532 amino-acid residues lacking the C-terminal half of the transmembrane domains and the entire C-terminal intracellular domain. We isolated kidneys from *Pkd1*$^{del34/del34}$ or wild-type E15.5 embryos, dissociated them with collagenase and plated them out in Dulbecco's modified Eagle medium containing 2% fetal bovine serum, 0.75 μg l^{-1} interferon-γ, 1.0 g l^{-1} insulin, 0.67 mg l^{-1} sodium selenite, 0.55 g l^{-1} transferrin, 0.2 g l^{-1} ethanolamine, 36 ng ml^{-1} hydrocortisone, 0.10 μM 2,3,5-triido-L-thyronine, 100 units penicillin-G (base) in combination with 0.30 mg ml^{-1} additional glutamine, 100 μg streptomycin sulfate and 0.1 mM citrate to maintain penicillin potency. We obtained all cell culture supplements from Invitrogen except for interferon-γ, hydrocortisone and 2,3,5-triido-L-thyronine, which we obtained from Sigma. We determined the genotypes of these cells as described previously[24]. For cell sorting, we grew cells to confluence for 3 d at 37 °C. After trypsinization, we incubated 10^6 cells ml^{-1} with 10 μg ml^{-1} DBA (Vector Lab) and carried out cell sorting as described[42]. We added 11.0 g l^{-1} sodium pyruvate to maintain cell viability in suspension media. We only used cells from passages 3–18 after sorting. Unless otherwise stated, we purchased all chemicals from Sigma.

Immunolocalization of PC1 and PC2. We sectioned mouse embryonic kidneys (E15.5) to a thickness of 5 μm and grew tubular epithelial cells to various degrees of confluence. After fixation, we incubated samples overnight at 4 °C with a purified antibody against PC1 (1:1,000 dilution) and then with secondary antibody against rabbit labeled with fluorescein isothiocyanate (1:500 dilution) for 1 h at room temperature. For double labeling, we co-labeled antibodies to the cilia markers α-tubulin or γ-tubulin (1:10,000) with the antibody against PC1 and then secondary antibody against mouse labeled with Texas Red (1:500 dilution) as described previously[28].

Ca^{2+} microfluorimetry. We grew epithelial cells for at least 2 d in the absence of interferon-γ to induce optimal differentiation. We formulated a non-fluorescent, CO_2-independent medium for Fura-2 Ca^{2+} imaging (pH 7.3), which contained 1.26 mM $CaCl_2$, 0.81 mM $MgSO_4$, 5.37 mM KCl, 0.44 0mM KH_2PO_4, 137 mM NaCl, 0.34 mM Na_2HPO_4, 5.55 mM D-glucose, 2.0 mM L-glutamine, 1.0 mM sodium pyruvate, 20.0 mM HEPES buffer and 1% bovine serum albumin. We used the same buffer without $CaCl_2$ and $MgSO_4$ as Ca^{2+}-free buffer with 1 mM of ethylene glycol tetra-acetic acid (EGTA). In some experiments, we incubated cells with caffeine (30 mM), ryanodine (30 μM), GDPβS (10 μM), U73122 (10 μM) or 2-APB (10 μM) for 45 min before flow activation. In other experiments, we incubated cells with antibodies against PC1 or PC2 at a dilution of 1:50 for at least 45 min. We then washed cells at least three times with phosphate-buffered saline.

The experimental setup for flow has previously been described in detail[21]. Briefly, we incubated cells for 30 min with the Ca^{2+} sensitive probe Fura2-AM (5 μM) at 37 °C. We then washed cells three times to remove excess Fura2-AM and placed them in a perfusion chamber with a thickness of 0.0254 cm and width of 1.0 cm (GlycoTech). The chamber was positioned under a Nikon Diaphot microscope equipped with a CCD camera using IPLab software for Macintosh. We captured paired Fura images every 5 s at excitation wavelengths of 340 nm and 380 nm. After equilibration in the microscopy media for at least 10 min, we then stimulated the primary cilia of these cells at a fluid shear stress of 0.75 dyne cm^{-2}. We radiometrically calculated the Ca^{2+} level relative to the baseline value using R_{min} and R_{max} values of 0.3 and 6.0, respectively.

Methods for quantification of agonist-induced Ca^{2+} influx and release have been described previously in detail[31]. Briefly, we loaded cells with 5 μM of Fura-2 AM (Molecular Probes) in HEPES buffer (pH 7.4) containing 132 mM NaCl, 4.2 mM $NaHCO_3$, 5.9 mM KCl, 1.4 mM $MgSO_4$, 1.2 mM Na_2HPO_4, 1.6 mM $CaCl_2$, 11 mM dextrose and 10 mM HEPES buffer. We removed $CaCl_2$ from the Ca^{2+}-free buffer and supplemented it with 1 mM EGTA. After equilibration for 15 min, we exposed cells to 1 μM of a hexapeptide thrombin receptor agonist (Bachem). The emitted fluorescence was filtered at 500 nm, and the ratio of the emitted light at excitation wavelengths 340 nm and 380 nm was calculated automatically as a measure of intracellular Ca^{2+}.

Generation of affinity-purified antibodies. To generate antibodies against PC1 or PC2, we used a segment of the extracellular first PKD domain of mouse PC1 (residues 866–882) for p96521 (ref. 43); part of the first extracellular loop of mouse PC2 (residues 278–428) for p57 and p58 (ref. 44); and the N-terminal intracellular tail of mouse PC2 (residues 44–62) for p96525 (ref. 45). We immunized New Zealand white rabbits with 0.1 mg of the corresponding synthetic peptides or affinity-purified, maltose-binding protein–polycystin fusion proteins (for p57 and p58). We purified all polyclonal antibodies using fusion protein- or peptide-bound affinity columns. Specificities of these antibodies were confirmed by western blotting or immunostaining; the PC1 antibodies recognized the same molecular-weight band on western blot and the same PC1-positive cells as a previously published antibody against PC1 (ref. 46). We created both PC1 and PC2 stable cell lines according to manufacturer's protocols (Invitrogen).

Electrophysiology. We carried out the electrophysiological studies using the outside-out mode of the patch-clamp technique. Pipette solution contained 100 mM KCl, 0.1 mM $CaCl_2$, 10 mM HEPES buffer, 5 mM EGTA, pH 7.5. When filled with this internal solution, the pipette tip resistances were 5–10 MΩ. We used seals with resistances of >5 GΩ in single-channel experiments and measured currents with an integrating patch-clamp amplifier. Single-channel currents were filtered at 3 kHz through an 8-pole Bessel filter. The bath solution contained 100 mM KCl, 10 mM HEPES buffer, pH 7.5. The voltages were applied and single-channel currents digitized (150 μs per point) and analyzed using Digidata converter and programs based on pClamp (Axon Instruments). We calculated open probability (Po) from 30-s segments of current records in patches containing only one functioning channel, because we observed only one current level in these recordings. We analyzed several hundred or more events using half-amplitude threshold criteria for generating each data point. The experiments were carried out at 23 °C. In about 20% of the recordings, we observed subconductance states and brief openings of the main conductance. Because the changes in the main conductance events were the most relevant effects of the antibodies, we excluded channel activity resulting from the substates and events shorter than 1 ms. We used K^+ rather than Ca^{+2} as the charge carrier, because K^+ produced larger current amplitudes that allowed us to achieve a more accurate measurement of the changes in the opening probability elicited by the antibodies.

Data analysis and statistics. We calculated cytosolic free Ca^{2+} concentrations using the formula $[\text{Cyt } Ca^{2+}] = K_d \times ((R - R_{min}) / (R_{max} - R)) \times (F_{max}$ at 380 nm / F_{min} at 380 nm) where K_d denotes apparent dissociation constant of Fura2 indicator (145 nM), R is the ratio of 510 nm emission intensity when excited at 340 nm to 510 emission intensity when excited at 380 nm, R_{min} and R_{max} are ratios at zero and saturating (10 mM) Ca^{2+} concentrations, respectively, and F_{max} and F_{min} are the fluorescence intensity excited at 380 nm at zero and saturating free Ca^{2+} concentrations, respectively. At the end of the Fura-2 experiments, we incubated cells with calcium-free solution containing 140 mM potassium, 2 mM EGTA and 10 μM ionomycin (at pH 8.6 to optimize the ionomycin effect) for about 5 min. This allowed us to obtain the minimum signal ratio and values of R_{min} and F_{max} at 380 nm. We then supplied excess Ca^{2+} to the cell by adding 10 mM $CaCl_2$ to determine the maximum signal ratio. After the 340-nm and 380-nm signals were stable (roughly 3 min), we obtained the values of R_{max} and F_{min} at 380 nm. All of the fluorescence measurements were then corrected for autofluorescence.

All values for statistical significance represent mean ± s.e., and each data set was verified to be normally distributed before analysis. We carried out comparisons between means using paired Student's *t*-test. For all comparisons, we carried out power analyses to enable reliable conclusion, and coefficient variances were below 10%. All comparisons with negative results had statistical powers of ≥0.8, and statistical significance implies $P < 0.05$.

Acknowledgments

We thank K.R. Spring, G.J. Pazour, M. Logman and G.B. Witman for discussions and Q. Xi and A.P. Wiebe for technical assistance. This work was supported by grants from the US National Institutes of Health (J.Z.), the US National Aeronautics and Space Administration (D.E.I.), a Howard Hughes Predoctoral Fellowship (F.J.A.) and a Polycystic Kidney Disease Foundation Postdoctoral Fellowship (S.M.N.).

Competing interests statement

The authors declare that they have no competing financial interests.

Received 29 July; accepted 9 December 2002.

1. Torres, V.E. Extrarenal manifestations of autosomal dominant polycystic kidney disease. *Am. J. Kidney. Dis.* **34**, xlv–xlviii (1999).
2. Calvet, J.P. & Grantham, J.J. The genetics and physiology of polycystic kidney disease. *Semin. Nephrol.* **21**, 107–123 (2001).
3. Stayner, C. & Zhou, J. Polycystin channels and kidney disease. *Trends Pharmacol. Sci.* **22**, 543–546 (2001).
4. Parnell, S.C. *et al.* The polycystic kidney disease-1 protein, polycystin-1, binds and activates heterotrimeric G-proteins *in vitro*. *Biochem. Biophys. Res. Commun.* **251**, 625–631 (1998).
5. Delmas, P. *et al.* Constitutive activation of G-proteins by polycystin-1 is antagonized by polycystin-2. *J. Biol. Chem.* **277**, 11276–11283 (2002).
6. Chen, X.Z. *et al.* Transport function of the naturally occurring pathogenic polycystin-2 mutant, R742X. *Biochem. Biophys. Res. Commun.* **282**, 1251–1256 (2001).
7. Gonzalez-Perret, S. *et al.* Polycystin-2, the protein mutated in autosomal dominant polycystic kidney disease (ADPKD), is a Ca^{2+}-permeable nonselective cation channel. *Proc. Natl. Acad. Sci. USA* **98**, 1182–1187 (2001).
8. Vassilev, P.M. *et al.* Polycystin-2 is a novel cation channel implicated in defective intracellular Ca^{2+} homeostasis in polycystic kidney disease. *Biochem. Biophys. Res. Commun.* **282**, 341–350 (2001).
9. Koulen, P. *et al.* Polycystin-2 is an intracellular calcium release channel. *Nat. Cell Biol.* **4**, 191–197 (2002).
10. Hanaoka, K. *et al.* Co-assembly of polycystin-1 and -2 produces unique cation-permeable currents. *Nature* **408**, 990–994 (2000).
11. Moyer, J.H. *et al.* Candidate gene associated with a mutation causing recessive polycystic kidney disease in mice. *Science* **264**, 1329–1333 (1994).
12. Hou, X. *et al.* Cystin, a novel cilia-associated protein, is disrupted in the cpk mouse model of polycystic kidney disease. *J. Clin. Invest.* **109**, 533–540 (2002).
13. Pazour, G.J., San Agustin, J.T., Follit, J.A., Rosenbaum, J.L. & Witman, G.B. Polycystin-2 localizes to kidney cilia and the ciliary level is elevated in orpk mice with polycystic kidney disease. *Curr. Biol.* **12**, R378–R380 (2002).
14. Yoder, B.K. *et al.* Polaris, a protein disrupted in orpk mutant mice, is required for assembly of renal cilium. *Am. J. Physiol. Renal Physiol.* **282**, F541–F552 (2002).
15. Sleigh, M.A., Blake, J.R. & Liron, N. The propulsion of mucus by cilia. *Am. Rev. Respir. Dis.* **137**, 726–741 (1988).
16. Perkins, L.A., Hedgecock, E.M., Thomson, J.N. & Culotti, J.G. Mutant sensory cilia in the nematode *Caenorhabditis elegans*. *Dev. Biol.* **117**, 456–487 (1986).
17. Brueckner, M. Cilia propel the embryo in the right direction. *Am. J. Med. Genet.* **101**, 339–344 (2001).
18. Pazour, G.J. *et al. Chlamydomonas* IFT88 and its mouse homologue, polycystic kidney disease gene *tg737*, are required for assembly of cilia and flagella. *J. Cell Biol.* **151**, 709–718 (2000).
19. Murcia, N.S. *et al.* The Oak Ridge Polycystic Kidney (orpk) disease gene is required for left–right axis determination. *Development* **127**, 2347–2355 (2000).
20. Pennekamp, P. *et al.* The ion channel polycystin-2 is required for left–right axis determination in mice. *Curr. Biol.* **12**, 938–943 (2002).
21. Praetorius, H.A. & Spring, K.R. Bending the MDCK cell primary cilium increases intracellular calcium. *J. Membr. Biol.* **184**, 71–79 (2001).
22. Davies, P.F. Flow-mediated endothelial mechanotransduction. *Physiol. Rev.* **75**, 519–560 (1995).
23. Tulis, D.A., Unthank, J.L. & Prewitt, R.L. Flow-induced arterial remodeling in rat mesenteric vasculature. *Am. J. Physiol.* **274**, H874–H882 (1998).
24. Lu, W. *et al.* Perinatal lethality with kidney and pancreas defects in mice with a targeted *Pkd1* mutation. *Nat. Genet.* **17**, 179–181 (1997).
25. Lu, W. *et al.* Comparison of *Pkd1*-targeted mutants reveals that loss of polycystin-1 causes cystogenesis and bone defects. *Hum. Mol. Genet.* **10**, 2385–2396 (2001).
26. Watanabe, M., Muramatsu, T., Shirane, H. & Ugai, K. Discrete distribution of binding sites for *Dolichos biflorus* agglutinin (DBA) and for peanut agglutinin (PNA) in mouse organ tissues. *J. Histochem. Cytochem.* **29**, 779–780 (1981).
27. Wu, G. *et al.* Somatic inactivation of *Pkd2* results in polycystic kidney disease. *Cell* **93**, 177–188 (1998).
28. Geng, L. *et al.* Identification and localization of polycystin, the *PKD1* gene product. *J. Clin. Invest.* **98**, 2674–2682 (1996).
29. Ong, A.C. *et al.* Coordinate expression of the autosomal dominant polycystic kidney disease proteins, polycystin-2 and polycystin-1, in normal and cystic tissue. *Am. J. Pathol.* **154**, 1721–1729 (1999).
30. Chou, C.L. & Marsh, D.J. Measurement of flow rate in rat proximal tubules with a non-obstructing optical method. *Am. J. Physiol.* **253**, F366–F371 (1987).
31. Nauli, S.M., Williams, J.M., Akopov, S.E., Zhang, L. & Pearce, W.J. Developmental

changes in ryanodine- and IP(3)-sensitive Ca^{2+} pools in ovine basilar artery. *Am. J. Physiol. Cell Physiol.* **281**, C1785–C1796 (2001).
32. Wilson, P.D. Polycystin: new aspects of structure, function, and regulation. *J. Am. Soc. Nephrol.* **12**, 834–845 (2001).
33. Cocks, T.M. & Moffatt, J.D. Protease-activated receptors: sentries for inflammation? *Trends Pharmacol. Sci.* **21**, 103–108 (2000).
34. Bogatcheva, N.V., Garcia, J.G. & Verin, A.D. Molecular mechanisms of thrombin-induced endothelial cell permeability. *Biochemistry Mosc.* **67**, 75–84 (2002).
35. Kim, K., Drummond, I., Ibraghimov-Beskrovnaya, O., Klinger, K. & Arnaout, M.A. Polycystin 1 is required for the structural integrity of blood vessels. *Proc. Natl. Acad. Sci. USA* **97**, 1731–1736 (2000).
36. Boulter, C. *et al.* Cardiovascular, skeletal, and renal defects in mice with a targeted disruption of the *Pkd1* gene. *Proc. Natl. Acad. Sci. USA* **98**, 12174–12179 (2001).
37. Muto, S. *et al.* Pioglitazone improves the phenotype and molecular defects of a targeted *Pkd1* mutant. *Hum. Mol. Genet.* **11**, 1731–1742 (2002).
38. Lu, W. *et al.* Late onset of renal and hepatic cysts in *Pkd1*-targeted heterozygotes. *Nat. Genet.* **21**, 160–161 (1999).
39. Weston, B.S. *et al.* Polycystin expression during embryonic development of human kidney in adult tissues and ADPKD tissue. *Histochem. J.* **29**, 847–856 (1997).
40. Ward, C.J. *et al*. Polycystin, the polycystic kidney disease 1 protein, is expressed by epithelial cells in fetal, adult, and polycystic kidney. *Proc. Natl. Acad. Sci. USA* **93**, 1524–1528 (1996).
41. Rossetti, S. *et al.* The position of the polycystic kidney disease 1 (*PKD1*) gene mutation correlates with the severity of renal disease. *J. Am. Soc. Nephrol.* **13**, 1230–1237 (2002).
42. DeMaria, M., Johnson, R.P. & Rosenzweig, M. Four color immunofluorescence detection using two 488-nm lasers on a Becton Dickinson FACS Vantage flow cytometer. *Cytometry* **29**, 178–181 (1997).
43. Lohning, C., Nowicka, U. & Frischauf, A.M. The mouse homolog of *PKD1*: sequence analysis and alternative splicing. *Mamm. Genome* **8**, 307–311 (1997).
44. Wu, G. *et al.* Molecular cloning, cDNA sequence analysis, and chromosomal localization of mouse *Pkd2*. *Genomics* **45**, 220–223 (1997).
45. Pennekamp, P. *et al.* Characterization of the murine polycystic kidney disease (*Pkd2*) gene. *Mamm. Genome* **9**, 749–752 (1998).
46. Ong, A.C. *et al.* Polycystin-1 expression in PKD1, early-onset PKD1, and TSC2/PKD1 cystic tissue. *Kidney Int.* **56**, 1324–1333 (1999).